List of Supplementary Materials:

Fig. S12: Heatmap of PPARα-mediated intestinal barrier genes induced by exposure to *L. plantarum* in chronic SIV infection.

Fig. S13: Fenofibrate prevented the HIV-induced decrease in basal respiration and spare respiratory capacity

Fig. S14: Effects of mitochondrial rescue compounds on oxygen consumption rate in Caco-2 cells treated with HIV gp120 and tat.

Fig. S15: ECAR measurement following Fenofibrate treatment.

Supplementary Materials:

Methods and Materials

Study Design

The objective of this study was to investigate the pathogenic mechanisms regulating intestinal epithelial barrier disruption in HIV infection using SIV-infected rhesus macaques and human intestinal epithelial cell cultures. This study explored strategies to rapidly repair gut epithelial barriers by using *Lactobacillus plantarum* NCIMB8826-MM24 and associated bacterial metabolites. A total of 16 rhesus macaques at the California National Primate Research Center were enrolled in the study as approved by IACUC, 12 of which were infected intravenously with SIVmac251 for 10 weeks and 4 of which were served as SIV-negative controls. Animals were randomly assigned to experimental groups prior to the beginning of the experiment and screened for previous gastrointestinal complications and infections. To translate our findings to HIV infection, retrospective gene expression data from gut biopsies from 15 HIV-infected and HIV-negative individuals were utilized. No animals or subjects were excluded from analysis, and no blinding was performed during experimental administration of treatments. Colonic epithelial

Caco-2 cell cultures were used to examine the pathogenic effects of HIV antigens on disruption of epithelial tight junctions and mitochondrial impairment. Tight junctions and the role of PPARα signaling was investigated using PPARα agonist (fenofibrate) to repair HIV-mediated epithelial barrier disruption. *In vitro* assessment of epithelial permeability, gene expression, and mitochondrial function were performed.

Intestinal loop procedure and sample collection

The ileum was ligated into approximately 4-6 cm intestinal loops with intervening 1 cm spacer loops. Intestinal loops were injected with 1mL sterile MRS broth or sterile MRS broth containing $1x10^9$ CFU of *L. plantarum* NCIMB8826-MM24. We performed randomization of ileal loop segments by utilizing three replicates of intestinal loops for administration of *L. plantarum* with three alternating control media loops. The order of segments was standardized among all animals and loops were sampled in triplicate to capture potential variability in responses along the ileum. Intestinal loops were collected approximately 5 hours following bacterial administration for detection of changes in gene expression, T cell subset distribution, metabolomic profile, and histopathology. Flow cytometric, RNA, immunohistochemical, mitochondrial, metabolomics, and microbial analyses were performed.

Viral load Measurements

Total RNA was isolated from plasma and gut tissues using RNeasy kit (Qiagen) followed by digestion with DNAse I (Invitrogen). SIV RNA loads in plasma and gut tissue samples were determined by real-time reverse transcription-PCR (RT-PCR) to cDNA using Supercript III. SIV gag sequences were detected with Taqman system using Applied Biosystems ViiA 7 detection and ViiA 7 RUO software (Applied Biosystem) analysis. Viral RNA copies/µg of total RNA or RNA copies/ml plasma were calculated against a standard curve.

Cell isolation and flow cytometry

Ileal gut tissues were placed in isolation media (RPMI-1640 supplemented with 10% fetal bovine serum), 100 U/mL penicillin, 100 U/mL streptomycin, and 1 mg/mL collagenase type IIb and rested overnight in culture media (RPMI-1640 supplemented with 15% FBS, 1% gentamycin, 100 U/mL penicillin, 100 U/mL streptomycin, 1% l-glutamine, 1% sodium pyruvate, 2.5% Hepes, and 0.5% amphotericin B) at 37°C. Cells were stained with Aqua LIVE/DEAD viability dye (Invitrogen) and cell phenotype markers CD3, CD4, and CD8. Cells were analyzed on a LSRII flow cytometer (BD Bioscience). A minimum of one million events was collected per sample. Data analysis was performed using FlowJo version 8.8.6 (TreeStar).

RNA extraction and microarray analysis

Total RNA was extracted (RNeasy RNA isolation kit, Qiagen, Valencia, CA) from ileal tissues as previously described (10.1371/journal.ppat.1004311). mRNA amplification, labeling, hybridization to rhesus macaque whole genome GeneChips© (Affymetrix, Santa Clara, CA), staining, and scanning (Affymetrix Gene Expression Analysis Technical Manual) were performed at the host microbe and systems biology core at the University of California, School of Medicine. A minimum fold-change of 50% (p-value ≤ 0.05) was used as inclusion criteria for identifying significant differentially expressed genes between experimental and control groups. These genes were then functionally categorized to identify enriched and depleted biological pathways using Ingenuity Pathway Analysis software (Ingenuity Systems Inc., Redwood City, CA). For qRT-PCR verification, gut tissues were homogenized using a sterile steel bead and TissueLyser II (Qiagen). Total RNA was isolated from the RNeasy kit (Qiagen). Extracted RNA was treated with DNase I (Invitrogen) prior to synthesis of cDNA using Superscript III

(Invitrogen). RT-PCR (Taqman) was performed on a ViiA7 detector using Taqman primer probes and the following housekeeping index (HKI): glyceraldehyde-3-phosphate dehydrogenase (GAPDH) and actin beta (ACTB).

Immunofluorescence and immunohistochemistry

All samples used were fixed in 4% paraformaldehyde (PFA) and embedded in paraffin. 5μm sections were hydrated in ethanol, blocked, and incubated in the following primary antibodies: 1:100 rabbit polyclonal anti- ZO-1 (Invitrogen), 1:400 mouse monoclonal anti-occludin, 1:400 purified mouse anti-e-cadherin (BD Biosciences), 1:100 mouse monoclonal anti-Ki67 (DAKO), 1:400 goat IgG anti-human IL-1β (R&D Systems). Slides were incubated in the following secondary antibodies: Alexa Fluor 488 donkey anti-rabbit, Alexa Fluor 555 donkey anti-goat, Alex Fluor 488 donkey anti-mouse IgG (Invitrogen). Nuclei were visualized using DAPI nucleic acid stain (Invitrogen) and slides were mounted using 20μl ProLong Gold Antifade Mountant (Thermo Fisher).

Confocal microscopy and Immunofluorescence image analysis

Confocal z-stacks were captured using a Leica SP8 STED 3x confocal microscope (Leica Microsystems, Germany) with a white light laser. A 63x/1.4NA oil immersion objective and maximal image size at 1248x1248 pixels were utilized for all acquisitions. Z-stacks were performed with a 0.3μ step size at 1.25x capturing full thickness of individual channels. Four images were selected at random and captured for quantitative analysis. All confocal images were analyzed on Imaris Version 8.2 for 3-D visualization. Images were thresholded to eliminate background fluorescence. All structures were modeled using an additional surface to include areas above a fixed voxel number. Sum fluorescence intensities and volume were calculated from our regions of interest, as demarcated from the apical end of the epithelial cell nuclei to the

edge of the brush border. Fluorescence intensities between treatment groups were statistically analyzed using a two-tailed Mann-Whitney test with a 95% confidence interval and considered statistically significant when $p<0.05$.

Transmission Electron microscopy

Ileal tissues were fixed using Karnovsky's fixative in 0.1M sodium phosphate buffer (Sorenson's). $1mm^3$ pieces were cut then washed with the same buffer then secondarily fixed with 1% OsO4 in 0.1M PO4 buffer for 2 hours. Dehydration was accomplished using ascending concentrations of acetone then infiltrated and embedded in an epoxy resin mixture. Approximately 60 to 80nm sections were cut of the selected areas with a diamond knife (Diatome, Hatfield, PA) and picked up on copper grids. The sections were stained with uranyl acetate and lead citrate before viewing on a FEI Talos 120C Transmission Electron Microscope (Hillsboro, OR). Digital images were taken with the FEI Ceta 4k x 4k CMOS camera.

Evaluation of mitochondrial mass and morphology by Fiji: For mitochondrial mass and morphology quantification, images (two per condition) were ran through the "Analyze Particles" feature of Fiji (ImageJ). The following mitochondrial parameters were recorded: area (μm^2, scale bar used as reference), major and minor axes (μm), aspect ratio (AR, major/minor axis), and circularity. For the latest parameter values of 0.0 and 1.0 indicated respectively a perfectly tubular and circular shape. Mitochondria with values < 0.6 were considered tubular; values > 0.6 were considered indicative of circular mitochondria.

Statistical analysis: The D'Agostino-Pearson test was used to assess for normality. Statistically significant differences among groups were evaluated by Kruskal-Wallis test, followed by Dunn's multiple comparisons test, using the GraphPad Prism software (v. 7.04).

Metabolomic Analysis

Intestinal loop contents were analyzed using the Metabolon LIMS system (Metabolon, Inc.). The resulting extract was divided into fractions for analysis using two separate reverse phase (RP)/UPLC-MS/MS methods with positive ion mode electrospray ionization (ESI), .RP/UPLC-MS/MS with negative ion mode ESI, and HILIC/UPLC-MS/MS with negative ion mode ESI. Several types of controls were analyzed alongside experimental samples, including a pooled matrix sample, extracted water samples, and a cocktail of QC standards. Instrument variability was determined by calculating the median relative standard deviation (RSD) for the standards that were added to each sample prior to injection into the mass spectrometers. Experimental samples were randomized across the platform run with QC samples spaced evenly among the injections.

Bacteriology

L. plantarum NCIMB8826-R, which is rifampicin resistant was quantified by colony-forming unit (CFU) enumeration on MRS agar containing rifampicin (Thermo Fisher Scientific, Waltham, MA, USA), 50 μg/mL.

Gut microbiota analysis

DNA was isolated from ileal tissues after incubation with *L. plantarum* and media control using the PowerSoil Kit (MoBio). Sample preparation and 16S rRNA sequencing was performed as previously described (10.1038/mi.2015.92).

Cell cultures

Caco-2 cells (passage 4) were purchased from American Type Culture Collection (ATCC) and maintained in culture medium MEM, Earle's with L-Glutamine (Thermo Fischer), 10% fetal bovine serum (Invitrogen), and 1% Anti-Anti (Thermo Fischer). Cells were kept at 37°C in a 5% CO_2 chamber and culture medium was changed every 2 days. Caco-2 cells were subcultured after partial digestion with 0.05% trypsin-EDTA (Thermo Fischer) and only cells from passages 10-25 were used for subsequent analysis.

A Milicell ERS-2 Electrical Resistance System (Millipore) was used to measure transepithelial electrical resistance (TEER) of Caco-2 monolayers. Cells were grown on a 10mm transwell with 0.4μm filter membrane (Corning). TEER measurements higher than 1000 Ω were used in cell culture treatments.

For immunostaining analysis, Caco-2 cells were grown on a 24-well plate with 12mm Poly-D-Lysine/Laminin-coated glass coverslips (Corning). Cells reached confluence and were treated before fixation in 4% paraformaldehyde. Caco-2 cells were blocked in 15% donkey serum in PBS and incubated in 1:50 rabbit anti-human ZO-1 (Invitrogen) primary antibody overnight, followed by secondary antibody donkey anti-rabbit Alexa Fluo 488 for 1 hour. Nuclei were visualized using a DAPI nuclear stain (Invitrogen). Glass coverslips were removed from wells and mounted using Prolong Diamond Anti-fade. Images were captured at 63X using an LSM800 Zeiss laser scanning confocal microscope (Carl Zeiss, Oberkochen, Germany) and Zen 2009 Software (Zeiss).

For gene expression analysis, total RNA was isolated from Caco-2 cells using the RNeasy kit (Qiagen). Extracted RNA was treated with DNase I (Invitrogen) prior to synthesis of cDNA using Superscript III (Invitrogen). RT-PCR (Taqman) was performed on a ViiA7 detector using

the glyceraldehyde-3-phosphate dehydrogenase (GAPDH), carnitine palmitoyltransferase IA (CPT1A), Acyl-coenzyme A oxidase 1 (ACOX1), apolipoprotein A4 (APOA4), peroxisome proliferator-activated receptor alpha (PPARα), and pyruvate dehydrogenase kinase 4 (PDK4) Taqman primer probes.

Oxygen Consumption Rates (OCR) and Extracellular Acidification Rate (ECAR) using Seahorse XFe24

To measure OCR and ECAR, 200,000 Caco-2 cells (ATCC) were seeded in each well on a 24-well plate (Seahorse Biosciences, Billerica, MA) in MEM with 10% FBS and incubated overnight. Prior to analysis, media was changed to the un-buffered equivalent MEM media containing 2.0mM L-Glutamine without phenol red or sodium bicarbonate. Cells were equilibrated for 20 minutes prior to measurements. ECAR was recorded in mpH per minute and OCR was recorded in oxygen consumption per minute in pmol (pmol/min) using a Seahorse XF-24 instrument at baseline and after addition of mitochondrial compounds: Oligomycin: 1μM, FCCP: 3μM, Rotenone and Antimycin: 1μM.

ATP Synthesis Assay

To measure Complex I and Complex II-driven mitochondrial ATP synthesis rate, an ATP-bioluminescence assay kit (Roche CLS II) was used as previously published (10.1289/EHP1404). Caco-2 were permeabilized by incubating them with digitonin (4 μM) for 3 minutes and then the digitonin was aspirated out and the cells were washed twice with transportation buffer. Then the cells were incubated for 20 min in Buffer A supplemented with ADP 200 μM, Malate 5 mM and pyruvate 5 mM (Complex-I-driven assay) or succinate 5 mM

(Complex II-driven assay). The luminescence was measured after 20 min and the ATP concentration in each well was calculated from a standard curve.

Mitochondrial ROS Production

Mitochondrial superoxide production was evaluated essentially as previously described (10.1042/BCJ20170632) (10.3389/fgene.2018.00338) Caco2 cells (passage 17, 2.5×10^5) were seeded on sterile poly-lysine coated cover slips (Corning), grown at 37°C, and treated with HIV gp120 (0.1 μg/ml) + Tat (1.4μg/ml) and cell-free *L. plantarum* supernatant (10%) titrated to pH 7.5. Cells were subsequently incubated for 10 min at 37°C with 5 μM MitoSOX (ThermoFisher Scientific), prepared as per manufacturer's instruction and diluted in growth media, washed 3 x 5 min with growth media and fixed in 4% formaldehyde in PBS. After 3 washes with PBS and 1 in water, cells were mounted on glass slides with Fluoromount-G mounting media with DAPI (Invitrogen). Caco2 cells pre-treated with either antimycin A (1 μM) or FCCP (0.1 μM) for 1 h were used, respectively, as positive and negative control.

Images (15-20 fields for each treatment, correspondent to a minimum of 100 cells analyzed) were obtained with an Olympus FV1000 laser scanning confocal microscope (excitation and emission wavelengths 594 and 660 nm) at 40× magnification and a zoom = 2.5. Analysis of fluorescence intensity was carried out with Fiji and normalized by cell area.

Statistical Analysis

Graphpad Prism 7 was used for statistical analysis and data plotting. Significant differences between 3 or more groups were determined using a Kruskal-Wallis one-way analysis of variance (ANOVA) test followed by a post-hoc Dunn's Multiple Comparison Test. Comparisons of 2 groups were analyzed using a two-tailed Mann-Whitney test with a 95% confidence interval and

considered statistically significant when $p<0.05$. For metabolomics analysis of luminal contents, statistical analysis was performed using Kruskal-Wallis one-way analysis of variance corrected for false discovery rate (FDR) and classification analysis in ArrayStudio on log transformed data. Since the sample size across the experimental groups was variable, statistical analysis was performed using a mixed model ANOVA to incorporate repeated sampling into the statistical model. Fold-change is based on the least squares (LS) Means, and significance was determined when $q<0.25$ and $p<0.05$. Cell culture experiments were performed in at least 3 independent experiments. Measurements of OCR were statistically analyzed used a two-way ANOVA for treatment, time, and their interactions, followed by a Bonferonni post-hoc test. Significance was determined when $p<0.05$.

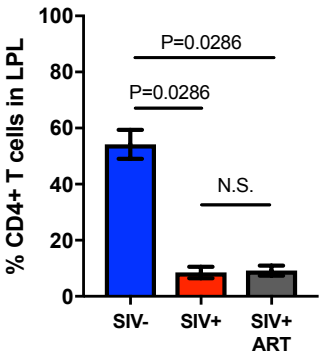

Fig. S1: Depletion of CD4$^+$ T cell percentages in lamina propria lymphocytes of SIV infected and ART treated macaques (n = 4 SIV-, n = 3 SIV+, n = 5 SIV+ART)**.**

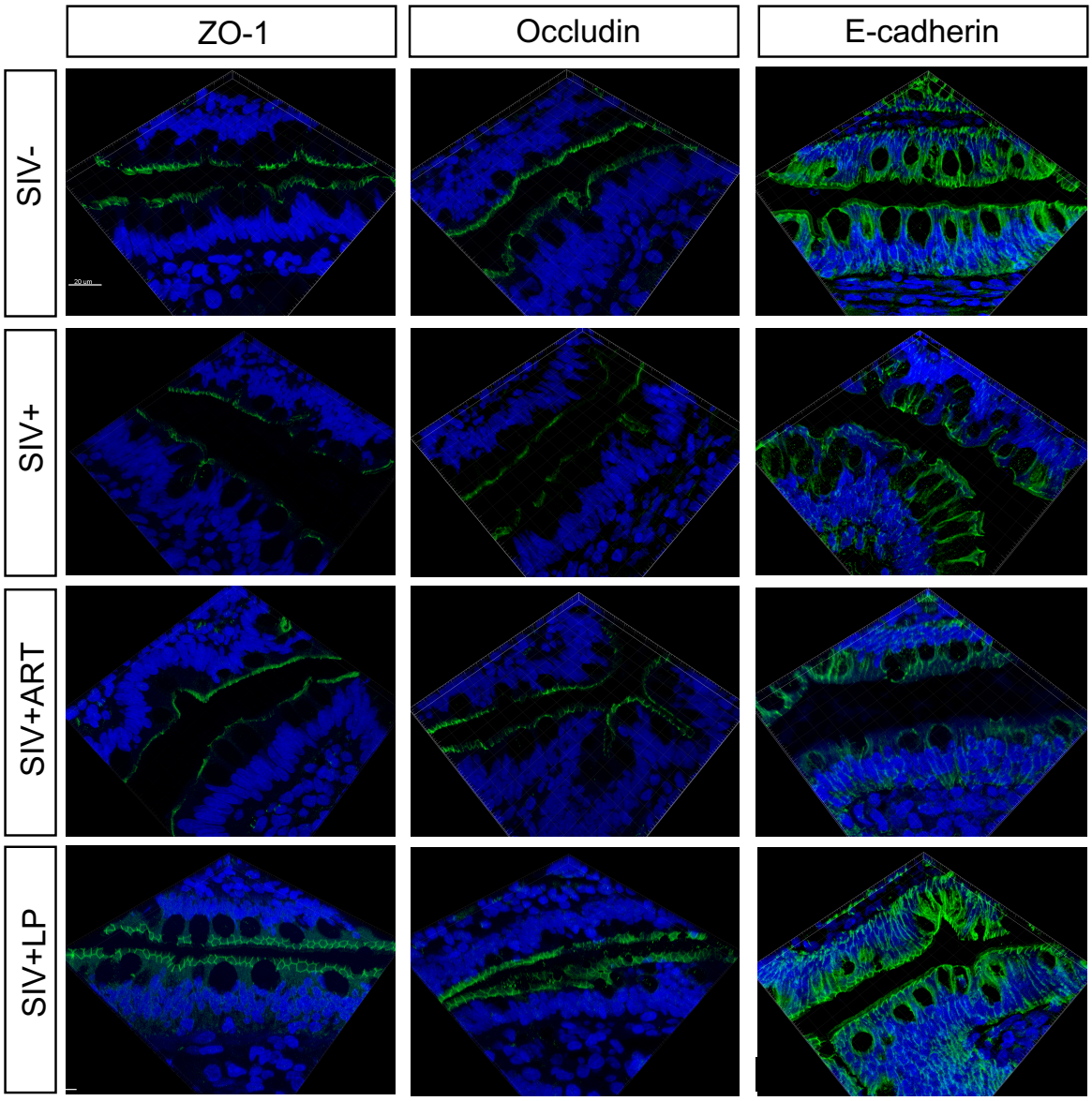

Fig. S2: Intestinal epithelial tight junction protein expression and distribution in SIV-infected and uninfected macaques. Ileal tissues from SIV+ macaques that received late ART or *L. plantarum* were compared to untreated SIV+ macaques and SIV- controls. Immunofluorescent images of ZO-1, occluding, and e-cadherin show reduction of tight junction protein distribution in SIV infection that is unresolved in late ART treatment but rapidly repaired after *L. plantarum* administration.

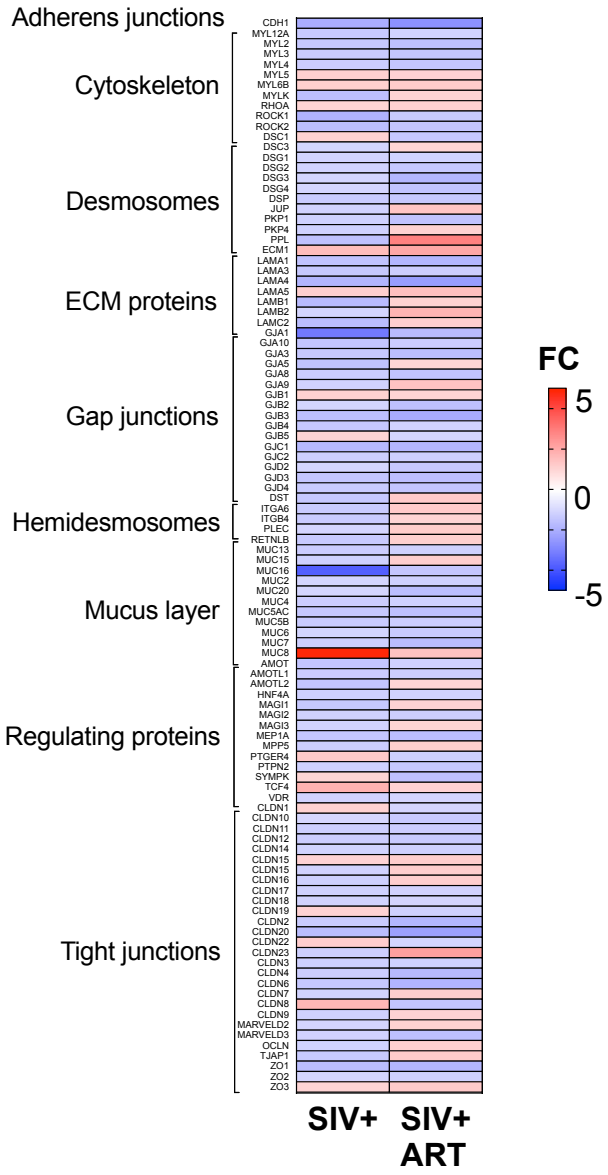

Fig. S3: Heatmap of genes involved in intestinal barrier permeability, secretory capacity, and absorptive enzymes. Heatmap of genes involved in intestinal barrier permeability, secretory capacity, and absorptive enzymes showed that late ART did not completely restore gut function at the transcriptome level.

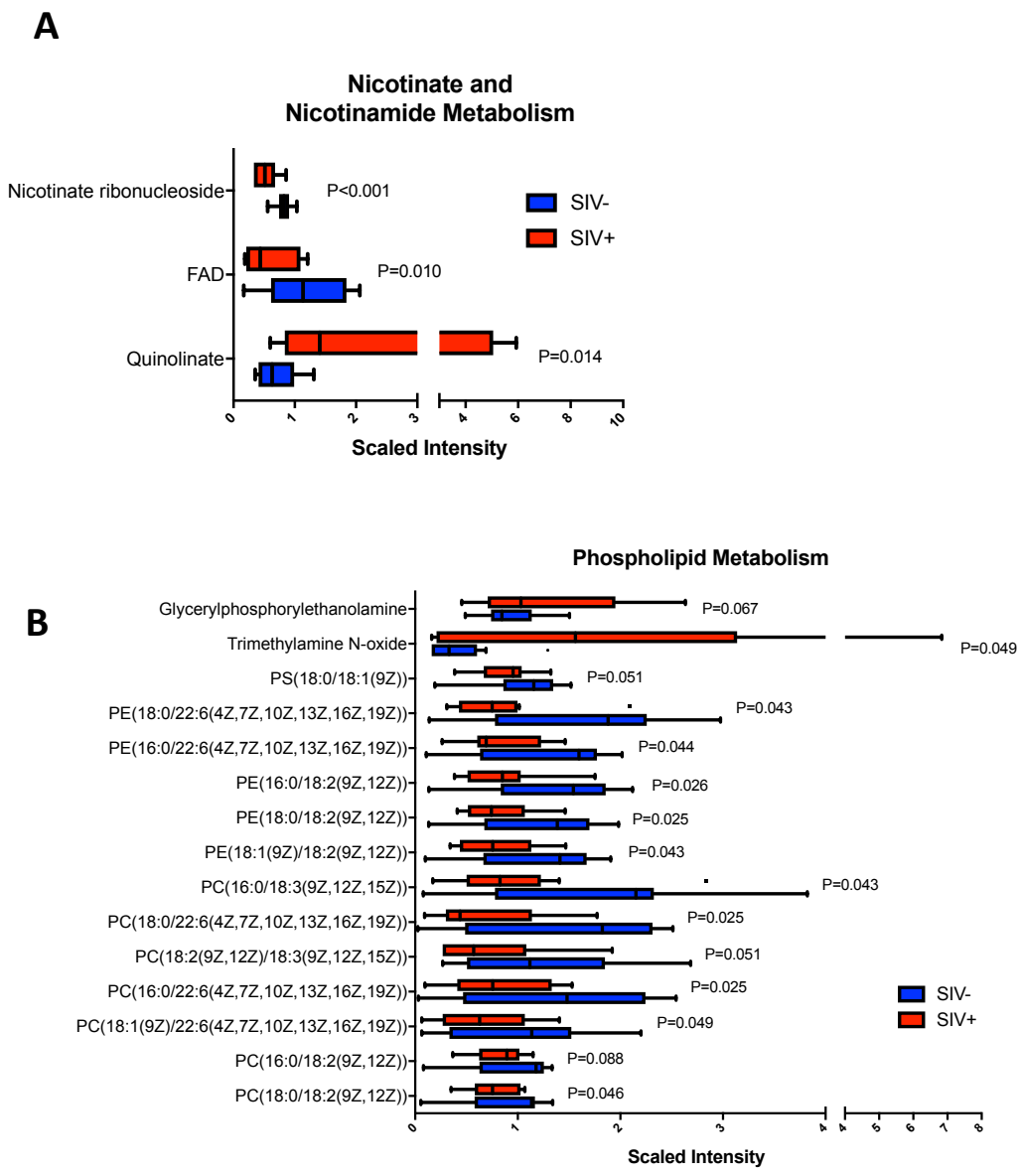

Fig. S4: Altered NAD and phospholipid metabolism in the gut between SIV-infected and uninfected controls. Quantitative levels of (**A**) nicotinate and nicotinamide metabolites and (**B**) phospholipid metabolites between SIV-infected macaques (n = 4) and healthy controls (n = 4) were measured using UPLC-MS/MS.

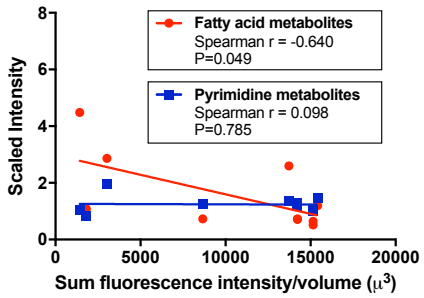

Fig. S5: Correlation between fatty acid metabolites and ZO-1 fluorescence intensity during SIV infection. Significant increases in short and medium chain acylcarnitines were detected in chronic SIV infection and were significantly correlated with tight junction protein ZO-1 fluorescence intensity on immunohistochemistry.

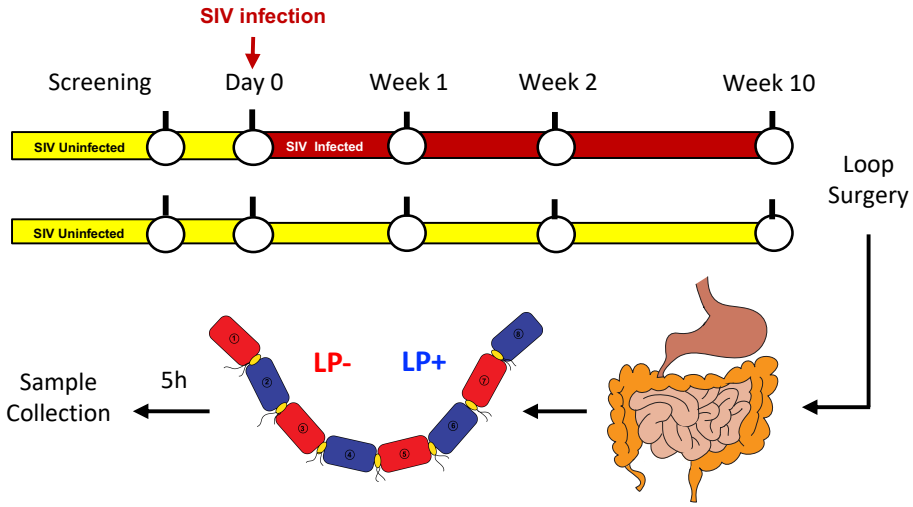

Fig. S6: An illustration depicting experimental administration of L. plantarum in intestinal loops of SIV-infected macaques (n = 4) and healthy controls (n = 4). controls.

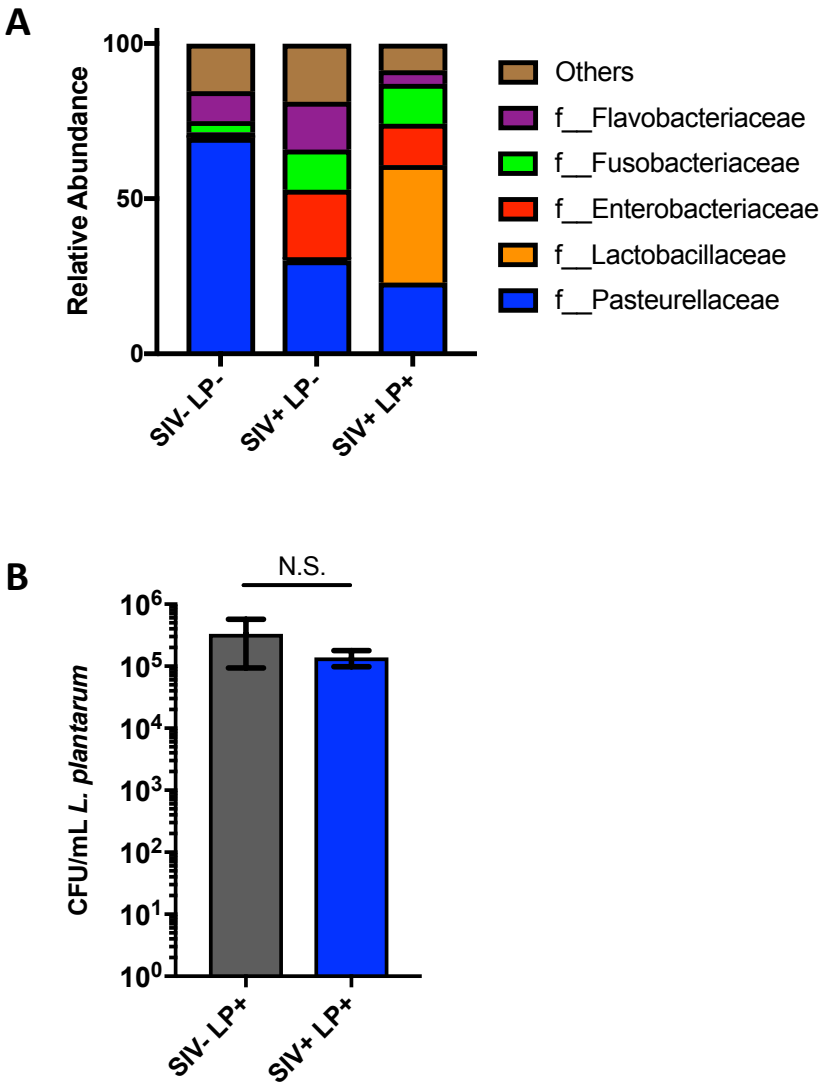

Fig. S7: Detection of *L. plantarum* following intestinal loop administration. Viability and presence of *L. plantarum* was measured by (**A**) 16S rRNA sequencing of ileal tissue and (**B**) colony-forming unit (CFU) enumeration on MRS agar after 5h incubation in intestinal loops.

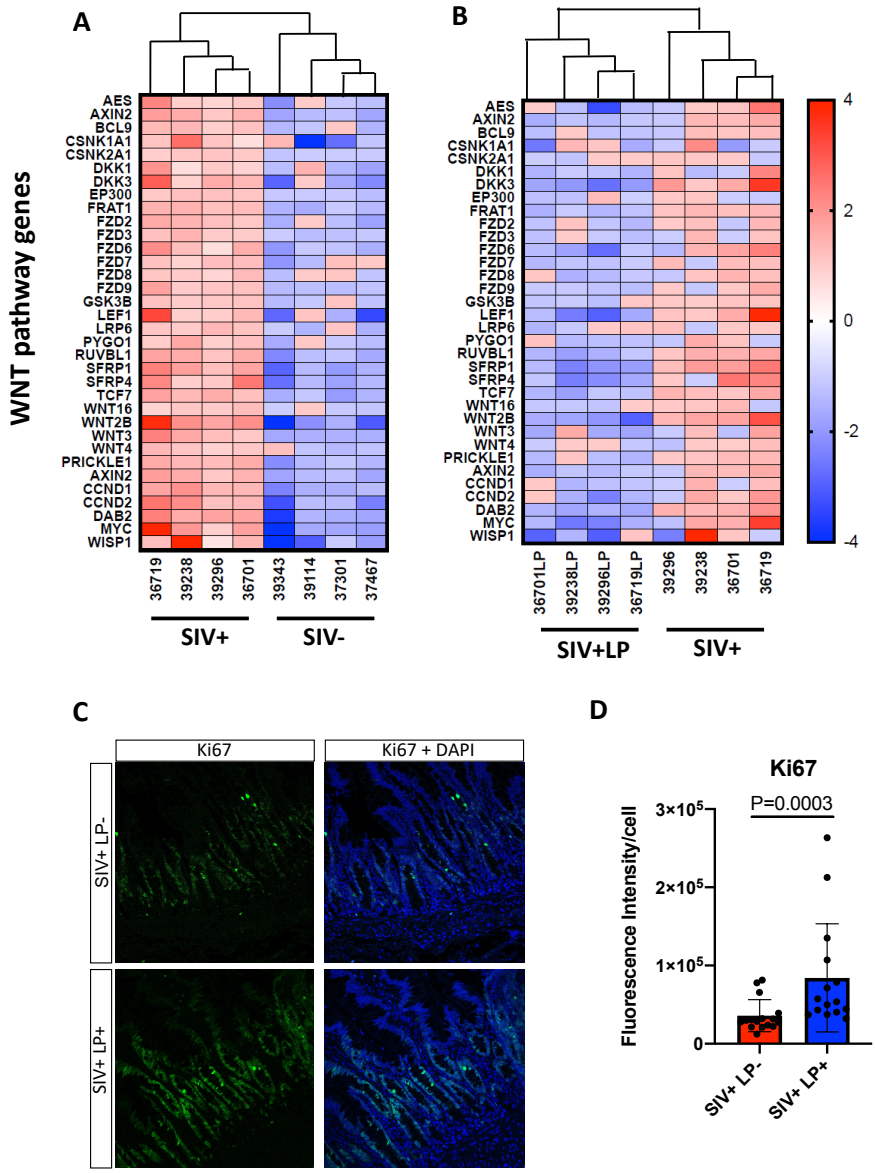

Fig. S8: Cell proliferative responses in WNT signaling to SIV infection following administration of *L. plantarum*. (**A**) Induction of WNT pathway in SIV infection and (**B**) reduction of WNT pathway after exposure to *L. plantarum* in the gut mucosa was identified by DNA microarray analysis of ileal tissue. (**C**) Immunofluorescent staining of Ki67 in ileal loops revealed enhanced cell proliferation following administration of *L. plantarum* as (**D**) quantified by fluorescence intensity/cell.

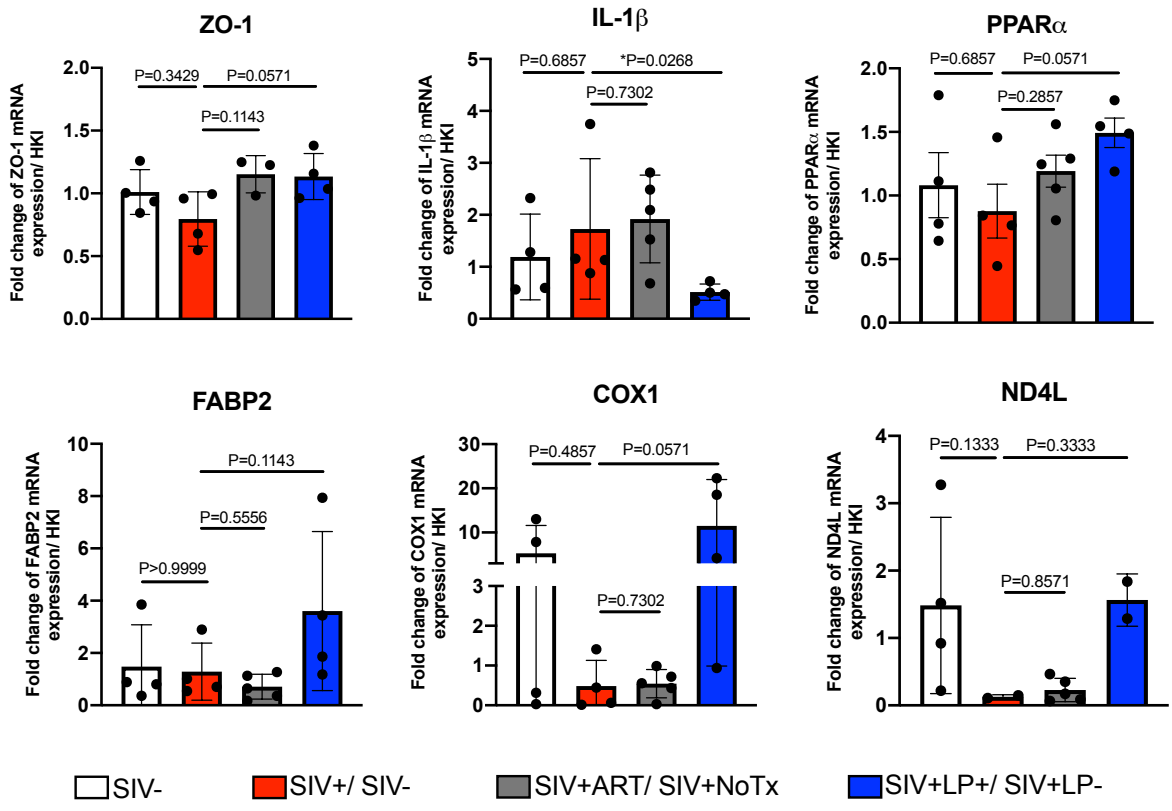

Figure S9: Gene expression analysis of ileal tissues by qRT-PCR. RNA was isolated from SIV-infected macaques treated with ART (*n=5*) or *L. plantarum* (*n=4*) compared to SIV-infected (*n=4)* and uninfected controls (*n=4*). Analysis of tight junctions (ZO-1), IL-1β, fatty acid metabolism (PPARα, FABP2), and mitochondrial function (COX1, ND4L) were used to verify trends in obtained by DNA microarrays. Statistical analysis was performed using a two-tailed Mann-Whitney test with a 95% confidence interval and considered statistically significant when $p<0.05$.

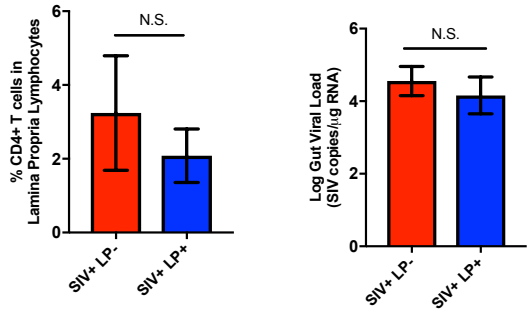

Figure S10: Gut viral loads and laminal propria CD4+ T cell percentages of intestinal loops after administration of *L. plantarum.* No detectable changes were observed in the gut viral loads and laminal propria CD4+ T cell percentages of intestinal loops after administration of L. plantarum as compared to untreated controls

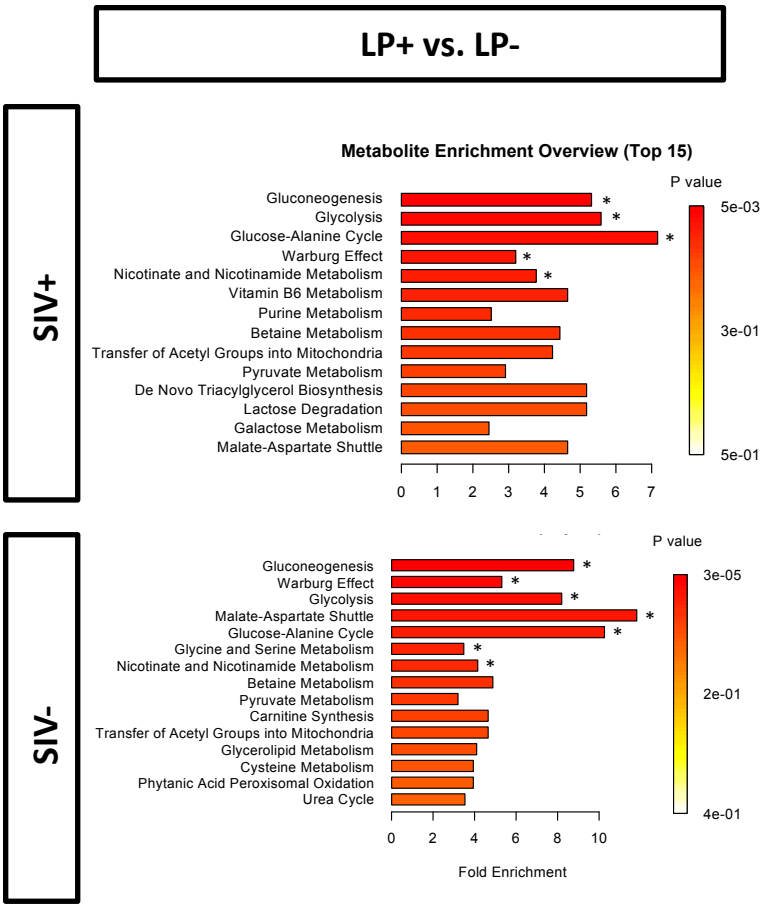

Fig. S11: Metabolomics enrichment analysis after exposure to *L. plantarum* in ileal contents from SIV-infected macaques and healthy controls. Enrichment pathway analysis from all significantly altered metabolites (q<0.25, p<0.05) was performed using MetaboAnalyst (*p<0.05). Ileal loops from SIV-infected macaques were exposed to *L. plantarum* for 5h and compared to MRS media control (n = 4 in SIV+LP+ group, n = 4 in SIV+LP- group), while healthy control loops following *L. plantarum* were compared to MRS control (n = 4 in SIV-LP+ group, n = 4 in SIV-LP- group).

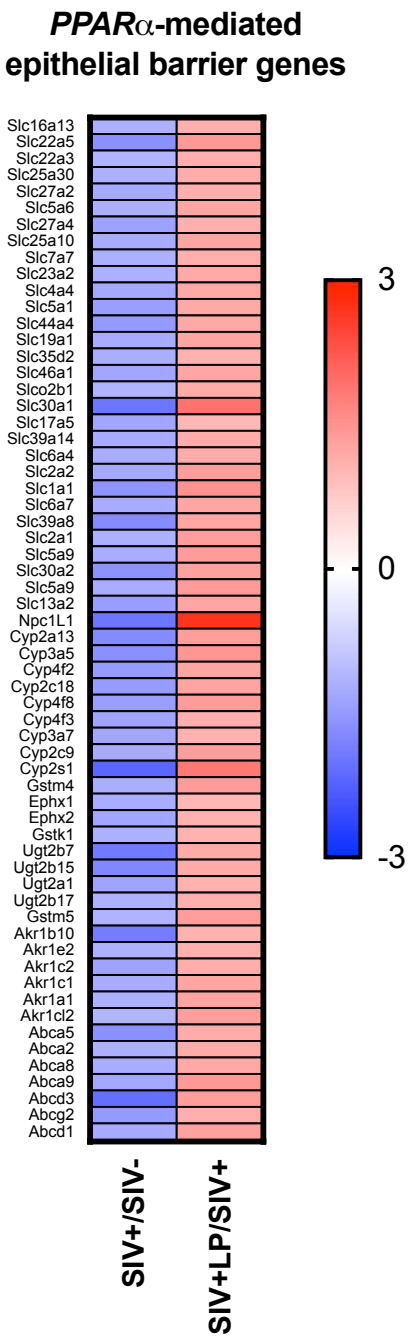

Fig. S12: Heatmap of PPARα-mediated intestinal barrier genes induced by exposure to *L. plantarum* in chronic SIV infection. Differential gene expression was measured using DNA microarray analysis from whole ileal tissue in healthy controls (n = 4) and SIV-infected macaques with and without administration of *L. plantarum* (n = 4 in SIV+ group, n = 4 in SIV+LP group)

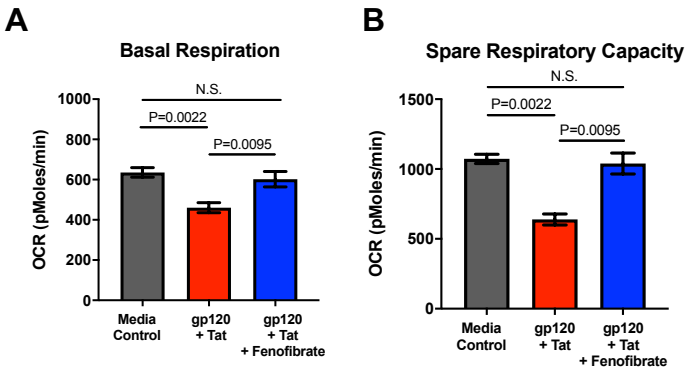

Fig. S13: Fenofibrate prevented the HIV-induced decrease in basal respiration and spare respiratory capacity. OCR was measured by Seahorse XFe24 after Caco-2 cells were pre-treated with fenofibrate (10μM) or DMSO for 1h before treatment with HIV gp120 (0.1 μg/ml) + Tat (1.4μg/ml) for 5h. Statistical analysis was performed using a two-way ANOVA and significant differences ($p<0.05$) were observed in mitochondrial (A) basal respiration and (B) spare respiratory capacity

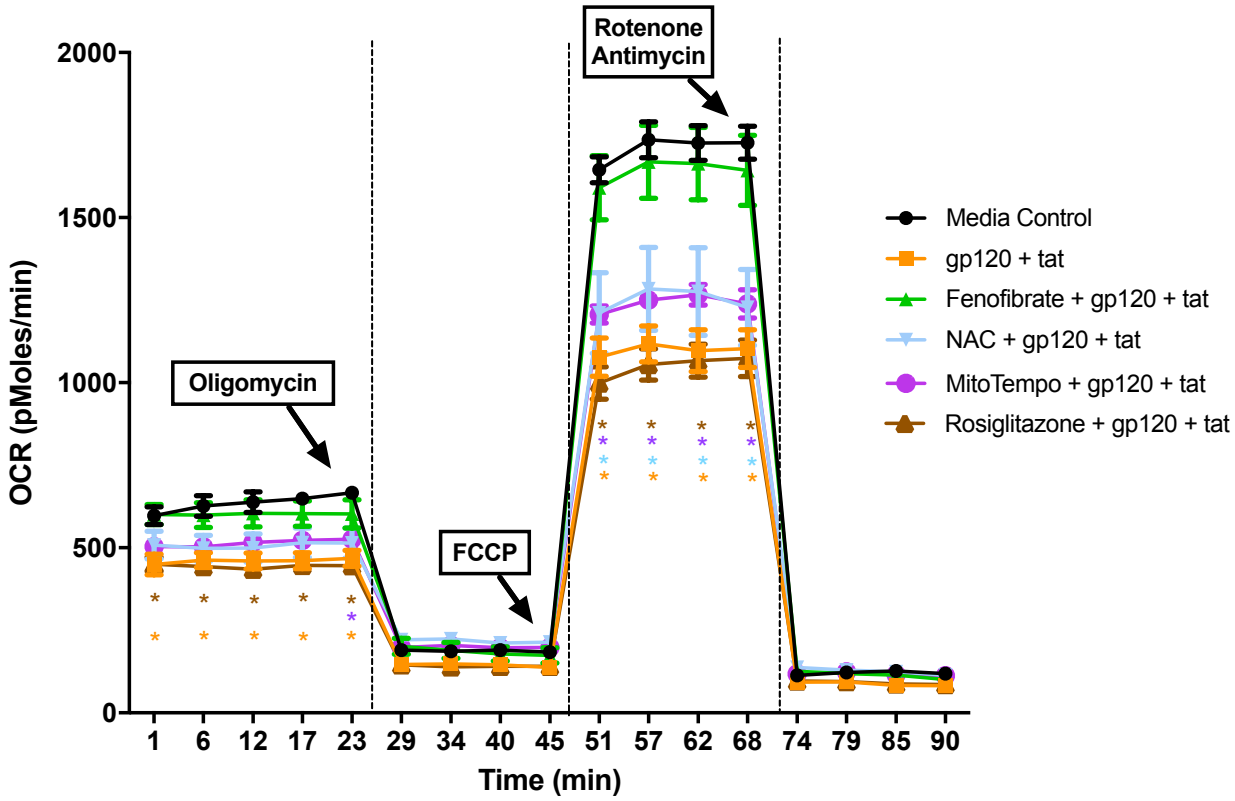

Fig. S14: Effects of mitochondrial rescue compounds on oxygen consumption rate in Caco-2 cells treated with HIV gp120 and tat. Mitochondrial respiration was measured on Seahorse XFe24 using Caco-2 cells pre-treated with fenofibrate (10μM), N-acetyl-cysteine (NAC, 500μM), MitoTempo (5μM), or the PPARγ agonist rosiglitazone (5μM) for 1h and subsequently treated with HIV gp120 (0.1 μg/ml) + tat (1.4μg/ml) for 5h.

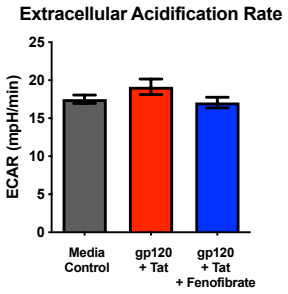

Fig. S15. ECAR measurement following fenofibrate treatment.

OCR was measured by Seahorse XFe24 after Caco-2 cells were pre-treated with fenofibrate (10μM) or DMSO for 1h before treatment with HIV gp120 (0.1 μg/ml) + Tat (1.4μg/ml) for 5h. Statistical analysis was performed using a two-way ANOVA and no significant differences ($p<0.05$) were observed following gp120, Tat, or fenofibrate treatment on ECAR.